

Morphological and Electrochemical Impedance Spectroscopy (EIS) Study of poly(3,4 ethylenedioxythiophene)-coated poly(acrylonitrile-*co*-styrene) nanoparticles

D.Gülercan¹ and A. S. Sarac^{2,*}

¹ Polymer Science and Technology, Istanbul Technical University, Maslak, Istanbul, Turkey

² Nanoscience & Nanoeng, Department of Chemistry, Istanbul Technical University, Maslak, Istanbul, Turkey

*E-mail: sarac@itu.edu.tr

Received: 24 June 2017 / Accepted: 26 October 2017 / Online Published: 1 December 2017

The nanoparticles of Poly(3,4-ethylenedioxythiophene)-coated Poly (acrylonitrile-*co*-styrene) (P(AN-*co*-St)/PEDOT) were successfully synthesized via a one-pot micro emulsion polymerization process. Ammonium persulfate (APS) and sodium dodecyl sulfate (SDS) were used to carry out the free-radical polymerization of P(AN-*co*-St) and the oxidative polymerization of 3,4-ethylenedioxythiophene (EDOT) monomer in microemulsion media. SEM, AFM, ATR-FTIR, UV-Visible were used to characterize their morphology and structure. High magnification SEM images of PEDOT-coated P(AN-*co*-St) nanoparticles obtained 25-65 nm. The results of ATR-FTIR and UV-visible spectrum revealed that the P(AN-*co*-St) nanoparticles are covered by PEDOT in the doped state. Electrochemical Impedance Spectroscopy (EIS) was used to indicate electrochemical performances of nanoparticles with time evolution. The electrochemical impedance spectroscopy data were fitted with Electrical Circuit Model of R(C(R(Q(R))))(CR) which gives a good correlation between the calculated and the experimental values. P(AN-*co*-St)/PEDOT nanoparticles exhibit capacitive behaviour similar to that of homo-PEDOT nanoparticle.

Keywords: Electrochemical impedance, Equivalent circuit model, Microemulsion polymerization; Nanocomposite; Poly(3,4-ethylenedioxythiophene).

1. INTRODUCTION

Micro emulsion polymerization has been improved to obtain nano-sized polymers. The particles are transferred into spherical aggregates toward the inside of the surfactant template with this process. Conducting polymer nanoparticles have been synthesized by some research groups, using

micro emulsion polymerization method. They reported particle sizes in the range of 50–200 nm [1,5]. There would be two purposes of utilizing the surfactant in the polymerization. The first one is the micelle formation that creates a micro-reactor vessel, where monomer is confined in a localized environment created from encapsulation by the surfactant. The second reason is to improve processibility of polymers and also physical properties of polymers such as solubility, stability and conductivity in organic solvents[6].

A standart micro-emulsion polymerization usually consists of monomer mixture, water, surfactant, initiator and co-stabilizer. The micro-emulsion polymerizations are more stable than the ordinary emulsion polymerization by thermodynamically and do not form any phase separation [7].

In recent studies, conducting polymers have been widely studied due to their interesting chemical and physical properties. Among conductive polymers, PEDOT is very special since it is easily synthesized and has lower band gap. The PEDOT has ability to reach high level doping due to its reactivity, thus more electrically conductive materials can be produced. The in situ oxidative emulsion polymerization process is a facile preparation method for the PEDOT nanoparticles since it provides separated nanomicelles. The nanomicelles contain organic phase that are dispersed in the aqueous medium, and the chemical oxidative polymerization of EDOT only takes place in the organic droplets [8].

Emulsion polymerization of pyrrole and thiophene derivatives using monomeric surfactants have been studied by a few research groups. For first time DeArmitt and Armes [9] described the colloidal dispersions of surfactant-stabilized polypyrrole particles in aqueous media using an anionic surfactant, sodium dodecylbenzenesulfonate (SDBS). They also investigated average particle size of nanoparticles 200-500 nm and also some polymerization conditions to obtain stable colloidal particles of polypyrrole. PPy and Polythiophene colloids have been synthesized by Oriakhi and Lerner [10] using a monomeric surfactant, SDBS. They described the formation of a large number of polymer latexes containing nanoparticles via emulsion polymerization. Kudoh synthesized PPy and PEDOT in aqueous solution using $\text{Fe}_2(\text{SO}_4)_3$ as oxidant and different monomeric surfactants. Although they obtained insoluble surfactant–oxidant complex, the nanoparticles represented approximately 40 and 60 S/cm conductivity values, respectively [11,12]. However, the nanoparticle sizes and morphologies have not been reported and particular clarification of the surfactant-oxidant complex effects on the high conductivity have not been explained in their study. Armes and coworkers reported the deposition of PEDOT onto near-monodisperse, micrometer-sized Polystyrene latexes. They also indicated that the optimum conducting polymer loading for well-defined PEDOT-coated PS latexes with reasonable solid-state conductivities (10^{-2} - 10^{-3} S cm^{-1}) [13]. Han et al. fabricated nanometre-sized PEDOT-silica core-shell particles and their corresponding hollow particles[14]. The monomer, 3,4-ethylenedioxythiophene (EDOT) is relatively insoluble in water and initiators react with water and the surfactant-free emulsion polymerization of EDOT leads to poor conductivity and low yields. To overcome this problem, it has been proposed that adding monomeric surfactants to an aqueous solution of EDOT monomer improves yield of polymerization significantly [15].

In this study, we successfully synthesized PEDOT nanoparticles on the prepared P(AN-co-St) matrix at appropriate monomeric surfactant concentration in aqueous solution. The micro emulsion

polymerization was chosen among various emulsion polymerization methods as the method could help us to obtain nano-sized polymer particles.

Sodium dodecylsulfate (SDS) was selected as surfactant dopant since it is not too expensive and commercially available. ATR-FTIR and UV-Visible were also used to investigate the characteristics of nanoparticles. The progress of polymerization followed by spectroscopic and morphologic measurements with respect to time.

Moreover, there are a few studies about electrochemical impedance measurement and electric circuit model of PEDOT coated nanoparticles, these measurements were also used to evaluate the time-dependent capacitive behavior of PEDOT-coated P(AN-co-St) nanoparticles.

2. EXPERIMENTAL

2.1. Materials

Acrylonitrile (AN), Styrene (St) was obtained from Sigma Aldrich. The initiator used for the polymerization was $(\text{NH}_4)_2\text{S}_2\text{O}_8$ (APS), Sodium dodecyl sulfate (SDS), methanol and ethanol were purchased from Merck reagents. EDOT was used an Aldrich reagent.

The characteristic functional groups of the samples were analyzed with Attenuated total reflectance Fourier transform infrared spectroscopy (ATR-FTIR) (PerkinElmer ATR-FTIR Spectrum One with a universal ATR attachment with a diamond and a ZnSe crystal, Shelton, USA). P(AN-co-St)/PEDOT and P(AN-co-St) polymers were characterized by UV-Visible (Perkin Elmer, Lambda 45) spectrophotometric analysis. P(AN-co-St)/PEDOT and P(AN-co-St) were dissolved %2 volume fraction in water for characterization by using UV-Visible spectrophotometer. Nanoparticles were characterized as morphological by Atomic Force Microscope (AFM) (Nanosurf EasyScan2 STM) and Scanning electron microscope (SEM). Electrochemical impedance spectroscopy (EIS) measurement of nanoparticles was analyzed in % 0.01M LiClO_4 solution on glass with a platinum wire as a counter electrode, and a Ag wire as a quasi-reference electrode by Parstat 2263 Electrochemical Analyser via electrochemical impedance spectroscopy measurement. The Nyquist, Bode Magnitude, Bode Phase and admittance data of the EIS was measured in the frequency range 0.01 Hz–100 kHz using Z SimpWin V3.10, AC-impedance data analysis software program.

2.2. Preparation of the P(AN-co-St)/PEDOT Nanoparticles

2.2.1. Synthesis of P(AN-co-St) Nanoparticles

Emulsion polymerization of P(AN-co-St) was conducted using Acrylonitrile and Styrene monomers (9:1 molar ratios) in the presence of monomeric surfactant (SDS) and initiator (APS) in 150 ml aqueous solution. For the first step, SDS was dissolved in 145 ml water and mixed with magnetic stirrer. Afterwards AN and St monomers dissolved in surfactant solution. The solution which contains monomers (AN and St) and surfactant was stirred and then was transferred to three neck flask and temperature was raised 70°C then APS solution was added. The temperature of synthesis was held at

70 °C during 3h. The obtained P(AN-co-St) latex was highly stable and precipitation was not observed even after centrifugation at 6000 rpm for 30 min.

2.2.2. Synthesis of P(AN-co-St)/PEDOT Nanoparticles

Aqueous micellar dispersion of P(AN-co-St) copolymer was prepared as mentioned section 2.2.1 and 10 ml of P(AN-co-St) micellar solution was taken, subsequently EDOT monomer was added and solubilized in the 10 ml of this micellar solution. The molar ratio of EDOT monomer was determined after several experiments and was added into for producing PEDOT coated P(AN-co-St) nanoparticles.

The 0.08g of $(\text{NH}_4)_2\text{S}_2\text{O}_8$ (APS) dissolved in 1 ml of distilled water and then was added directly to the mixtures and they were stirred for 24 h at 25 °C (Fig.1). The molar ratio of EDOT monomer to APS is 2,5. During this polymerization, same amount of samples were taken at several time intervals to verify the particle formation and growth mechanism.

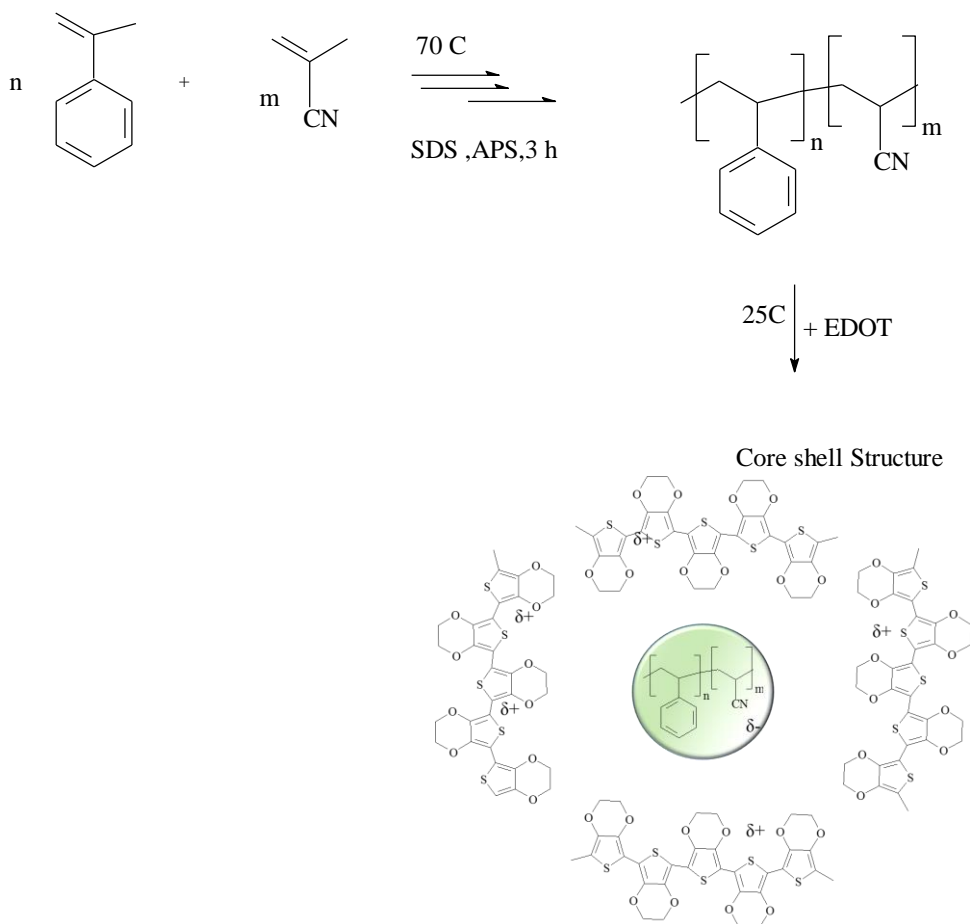


Figure 1. Schematic diagram for the synthesis of PEDOT on the P(AN-co-St) nanoparticles.

The nanoparticles were filtrated and then they were washed with deionized water and methanol/ethanol respectively, afterwards they were dried at $60\text{ }^\circ\text{C}$ for 24 h under vacuum. To investigate colloidal stability and morphologies of the particles, small amount of the samples were

taken from the washed products before drying process, they were re-dispersed in methanol for 10 min with ultrasonication.

3. RESULTS AND DISCUSSION

3.1. ATR-FTIR Spectrophotometric Characterization

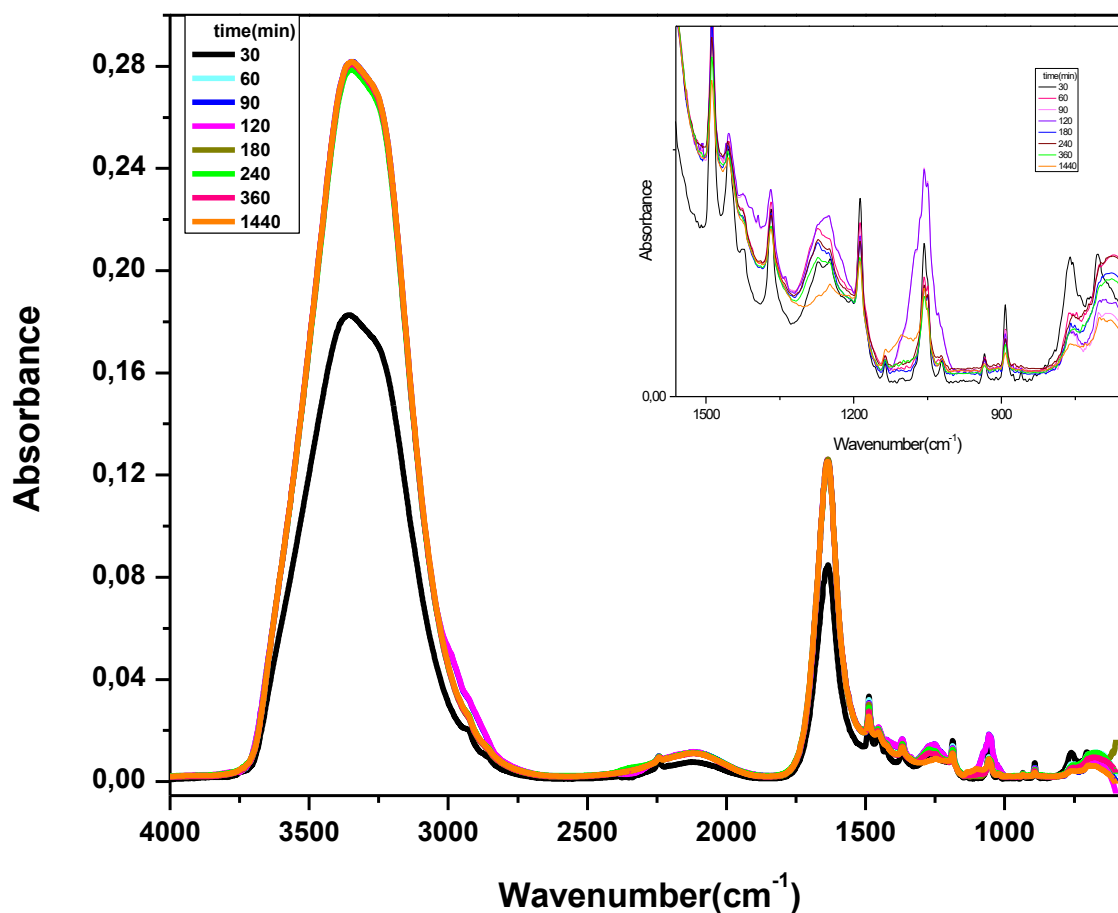


Figure 2. In situ ATR-FTIR spectra of P(AN-co-St)/PEDOT nanoparticles at various time intervals of polymerization.

For further confirmation, the growth of the PEDOT on P(AN-co-St) cores was examined by *in situ* ATR-FTIR analysis (Fig. 2). From the FTIR spectrum in Figure 2 the existence of a broad band between 2800 and 3700 cm^{-1} attributes the presence of -OH groups, which is caused by water solution medium during the synthesis. During the polymerization of EDOT in P(AN-co-St), C=C bonds disappear and are transformed into C-C single bonds. This transformation causes a new absorption bands at 1488 cm^{-1} . This characteristic peak of PSt which were referred to bending and stretching of sp^3 C-H bonds, absorbance value decreases with increasing time (Fig.4). Furthermore, the characteristic peaks at 705, 762 cm^{-1} of PSt disappears during polymerization. They can be attributed to the PEDOT formation on P(AN-co-St) core structure. The peak at 1635 cm^{-1} of APS overlaps with

both 1565 cm^{-1} characteristic peak of PSt and the characteristic peak of PEDOT at 1520 cm^{-1} . When APS is used as oxidant the existence of the peak at 1635 cm^{-1} (Fig. 2.) demonstrates the presence of C=O group, which can be ascribed to the overoxidation. Since EDOT has no free carbonyl group in its structure, the peak at 1635 cm^{-1} can confirm occurrence of overoxidation, as APS is a very strong oxidant. The conductivity can decrease by reason of overoxidation. The peaks 895 and 1187 cm^{-1} were caused from bisulfate ions. During the polymerization, bisulfate ion splits into sulfate ions, after polymerization the peaks at 895 cm^{-1} and 1187 cm^{-1} have not been observed due to the oxidized structure of PEDOT and not the other bisulfate peak expected at 1187 cm^{-1} [15,16].

The characteristic peak of PEDOT (inset graph of Fig.3) at 1368 cm^{-1} was ascribed to the inter-ring stretching mode of C–C and asymmetric stretching mode of C = C, this peak started to grow at 120 min. of the polymerization (Fig.3). It can be attributed that EDOT monomer was easily polymerized until 120.min and after this time PEDOT nanoparticles can be started to aggregation so that the characteristic peak of PEDOT (Fig. 3) at 1368 cm^{-1} decreases after 120 min.

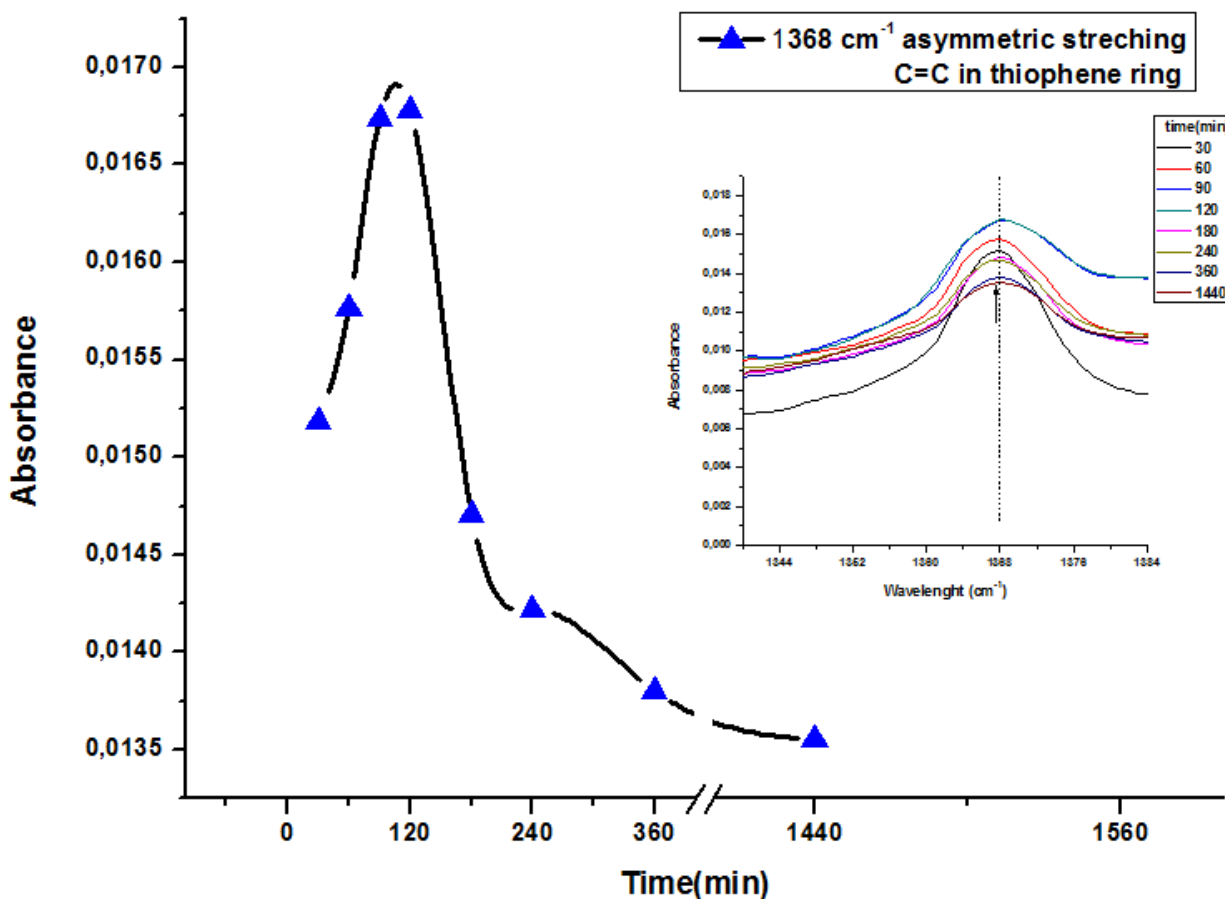


Figure 3. Absorbance-time curve for asymmetric stretching of C=C and inter-ring stretching of C-C at 1368 cm^{-1} for P(AN-co-St)/PEDOT nanoparticles, inset graph shows asymmetric stretching of C=C and inter ring stretching of C-C at 1368 cm^{-1} at various time intervals.

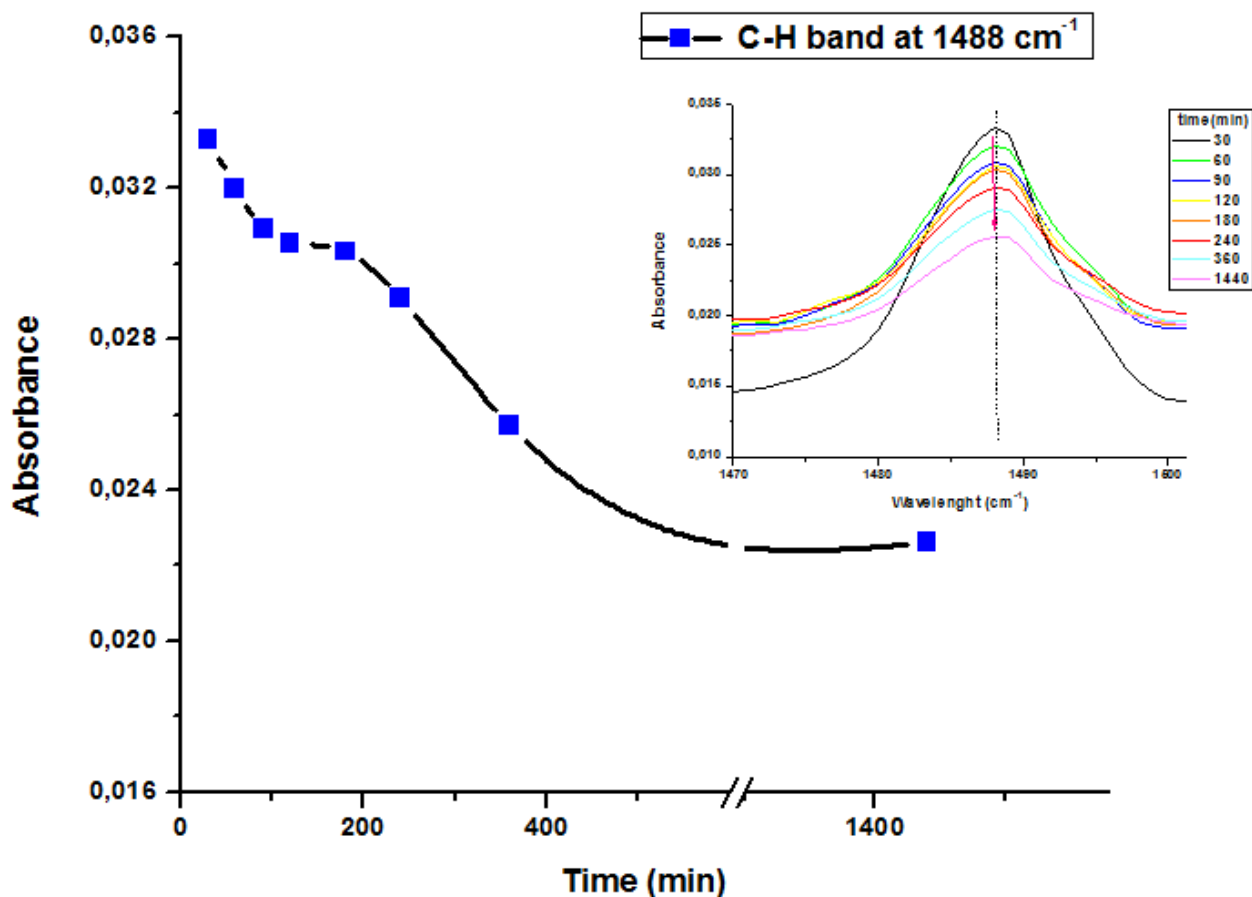


Figure 4. Absorbance-time curve for stretching and bending at 1488 cm^{-1} at various time intervals, inset graph shows stretching and bending of sp^3 of C-H in PSt.

In the Attenuated total reflectance Fourier transform infrared spectroscopy (ATR-FTIR) spectra of P(AN-co-St) and P(AN-co-St)/PEDOT (Fig.5), the characteristic absorption peaks at 2244 cm^{-1} and 1442 cm^{-1} related to the -CN stretching and -CH bending vibration of polyacrylonitrile, respectively. The peak at 2970 cm^{-1} confirm the transformation of C=C bonds into C-C single bonds; this is ascribed to the bending and stretching of sp^3 C-H bonds during the polymerization of styrene. The peaks at $813, 1016, 1126, 1192, 1225, 1424, 1571, 1846, 2008, 2663, 2824\text{ cm}^{-1}$ are characteristic for PEDOT composite[17]. The presence of the peaks at $1474, 1388\text{ cm}^{-1}$ (C=C and C-C stretching vibrations of the thiophene ring) are evidence of formation of the PEDOT in P(AN-co-St) /PEDOT. In our study, the FTIR spectrum of asymmetric stretching mode of C = C and inter-ring stretching mode of C-C band broadens and shifts to 1627 cm^{-1} . Ether bond stretching presents peaks at $1157, 1088, \text{ and } 1072\text{ cm}^{-1}$ in the ethylene dioxy group. The new peaks at $988, 927, 908, 879, 854 \text{ and } 689\text{ cm}^{-1}$ were indicated to C-S bond in the thiophene ring.

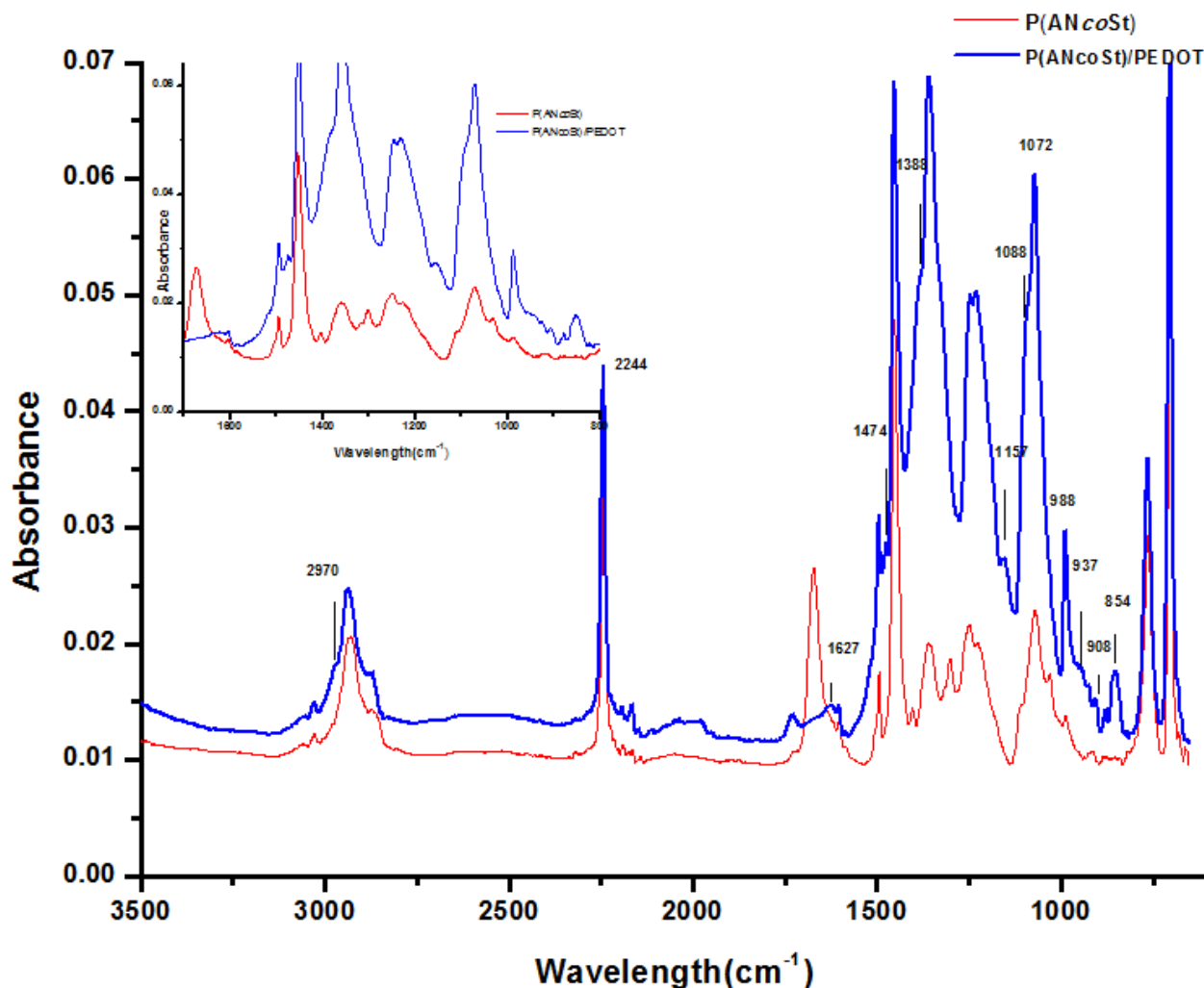


Figure 5. ATR-FTIR spectra of P(AN-co-St) and P(AN-co-St)/PEDOT from their solids form, inset graph shows the 800-1700 cm⁻¹ region.

3.2. UV-Visible Analysis

UV-Visible Spectra of P(AN-co-St) and P(AN-co-St)/PEDOT are shown in Fig.6. The progress of polymerization was followed by UV-Visible spectrophotometer while taking samples at time intervals (Fig. 7). Due to $\pi-\pi^*$ transition band of PEDOT, a peak around 770 nm, was observed. Also time-dependent polymerization was observed for changing absorbance of EDOT monomer between 220 - 350 nm by UV-Visible spectrophotometer (Fig.7).

There is a broad peak at 700 to 800 nm range. Neutral PEDOT has absorptions around 570 nm which is associated with the $\pi-\pi^*$ transition of neutral PEDOT. For oxidized PEDOT when conjugation length decreases which indicates the electronic delocalization decreases, the absorption can be around 700 nm to 900 nm which is attributed to bipolaron formation .

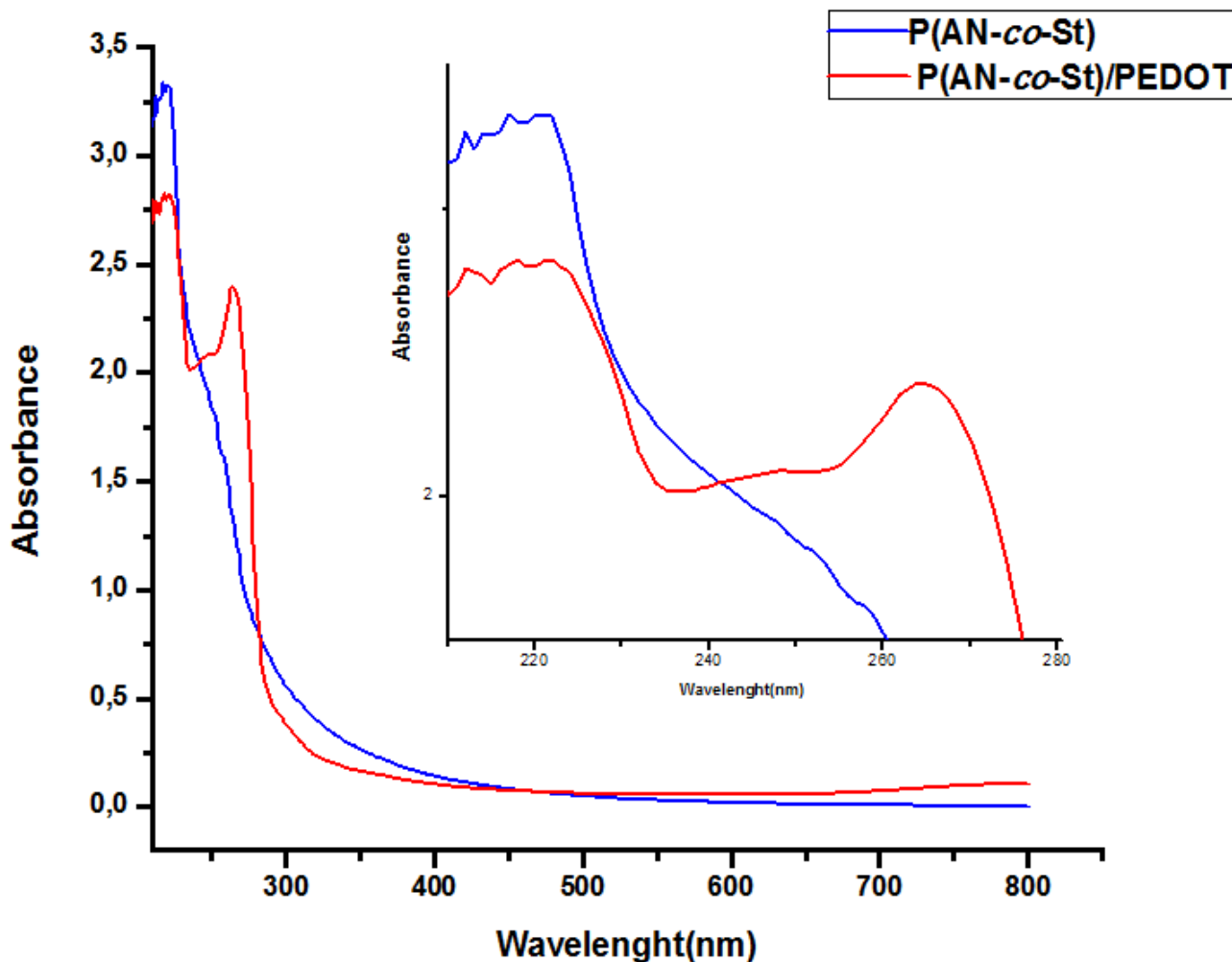


Figure 6. Comparison of absorbance results of P(AN-co-St) and P(AN-co-St)/PEDOT nanoparticles.

The UV-Visible spectra of samples exhibit absorption bands at 253 nm, due to $\pi-\pi^*$ transition of the aromatic group of the monomer repeat unit and side-chains. As the main-chain of the polymers have $\pi-\pi^*$ transition, absorption can be seen after 400 nm. At 770 nm, the absorbance exhibits a meaningful increase. The formation of polaronic charge carriers can be ascribed to this behavior. [18]

The absorbance increment at 770 nm is usually corresponding to radical-cations (polarons), while the optical density increasing at larger wavelengths (~ 1000 nm) is widely related with the dicationic (bipolaronic) form, also noticed in the PEDOT at similar wavelengths.[19]

It can be seen from Fig.8 the absorbance values at 580 and 770 nm are increasing but the absorption of monomer unit of EDOT at 253 nm is decreasing with time, it can be ascribed to the PEDOT formation on P(AN-co-St) core structure.

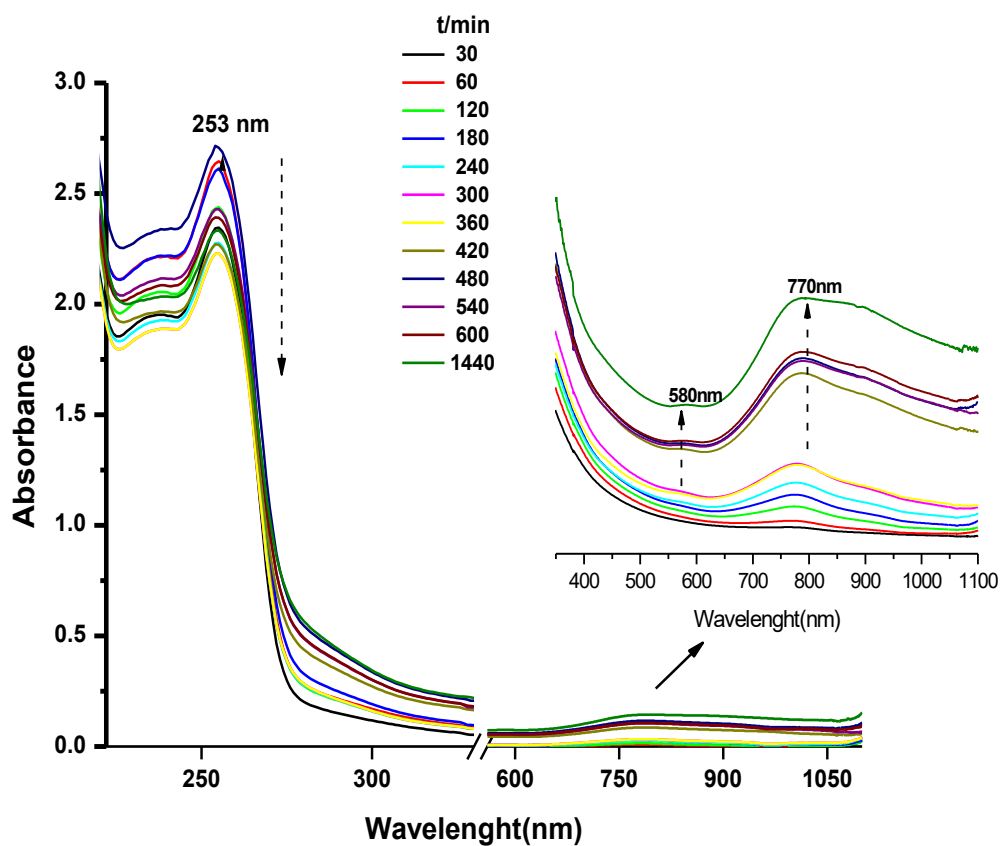


Figure 7. UV-Visible spectra, obtained at different times indicated, corresponding to aqueous micelleous P(AN-co-St)/PEDOT solution.

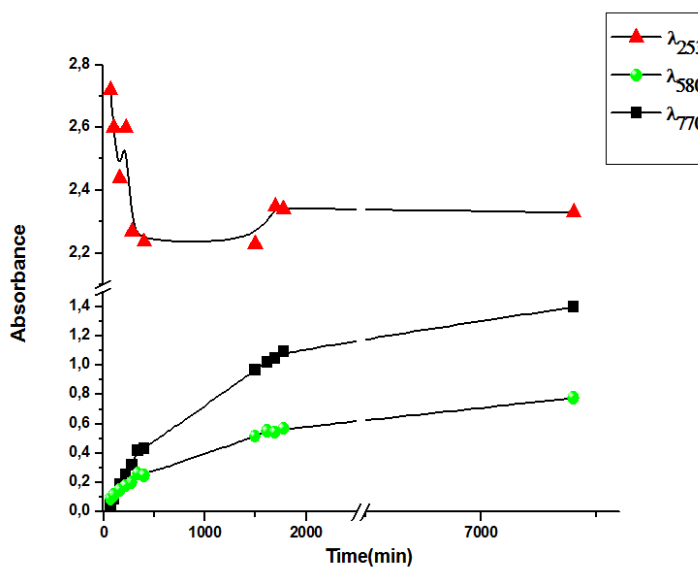


Figure 8. Change of absorbance values at 253, 580 and 770 nm with time for P(AN-co-St)/PEDOT aqueous micelleous samples.

3.3. Morphological Characterization of Nanoparticles

3.3.1. AFM Studies

To observe the surface morphology of nanoparticles were observed on mica glass surface by Atomic Force Microscopy. AFM analysis of P(AN-co St)/PEDOT on mica glass surface implied that nanoparticles were obtained throughout the polymerization process.

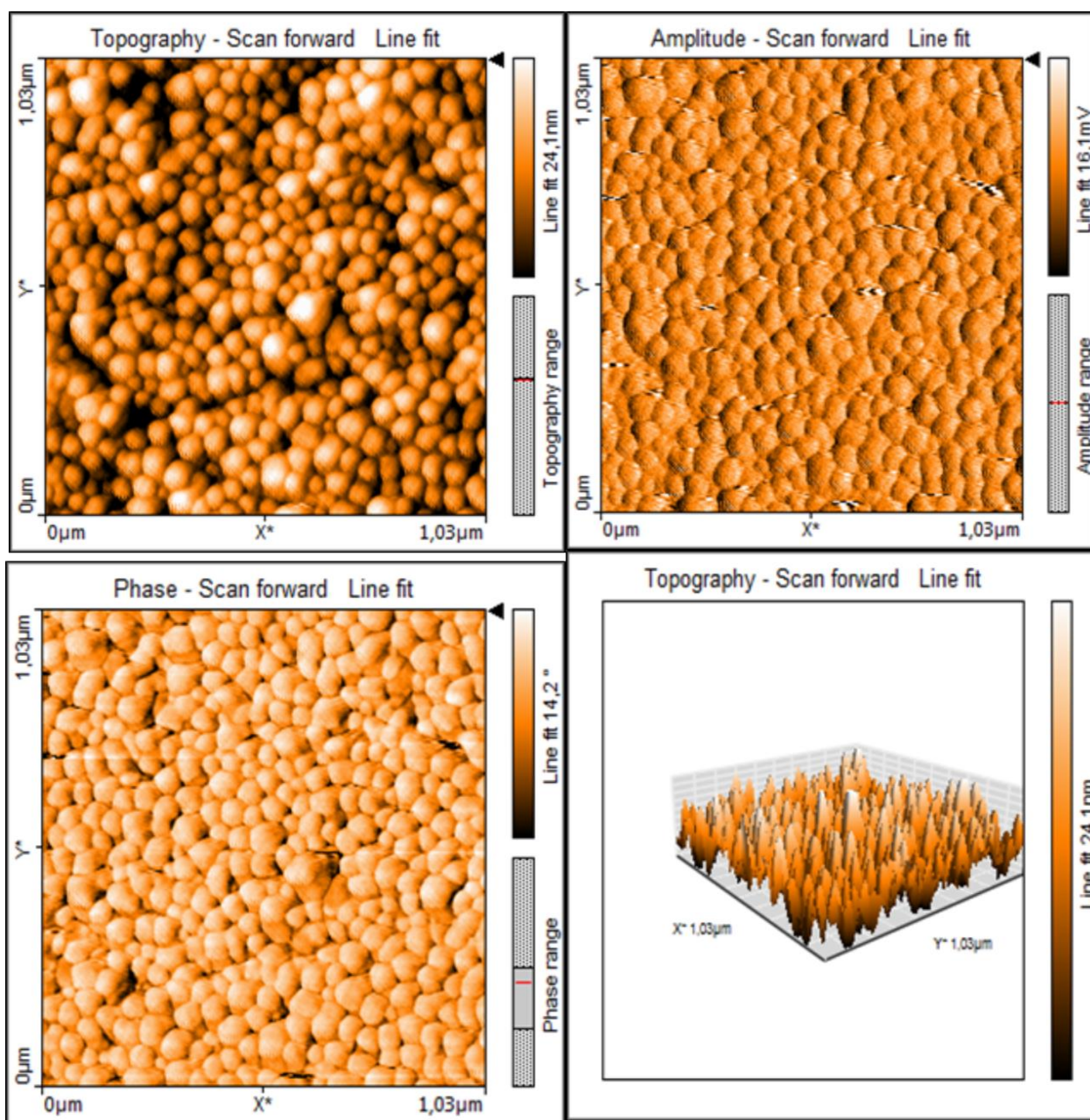


Figure 9. AFM image of P(AN-co-St)/PEDOT nanoparticles 1.03x1.03 μm area on mica glass surface, at 360min.

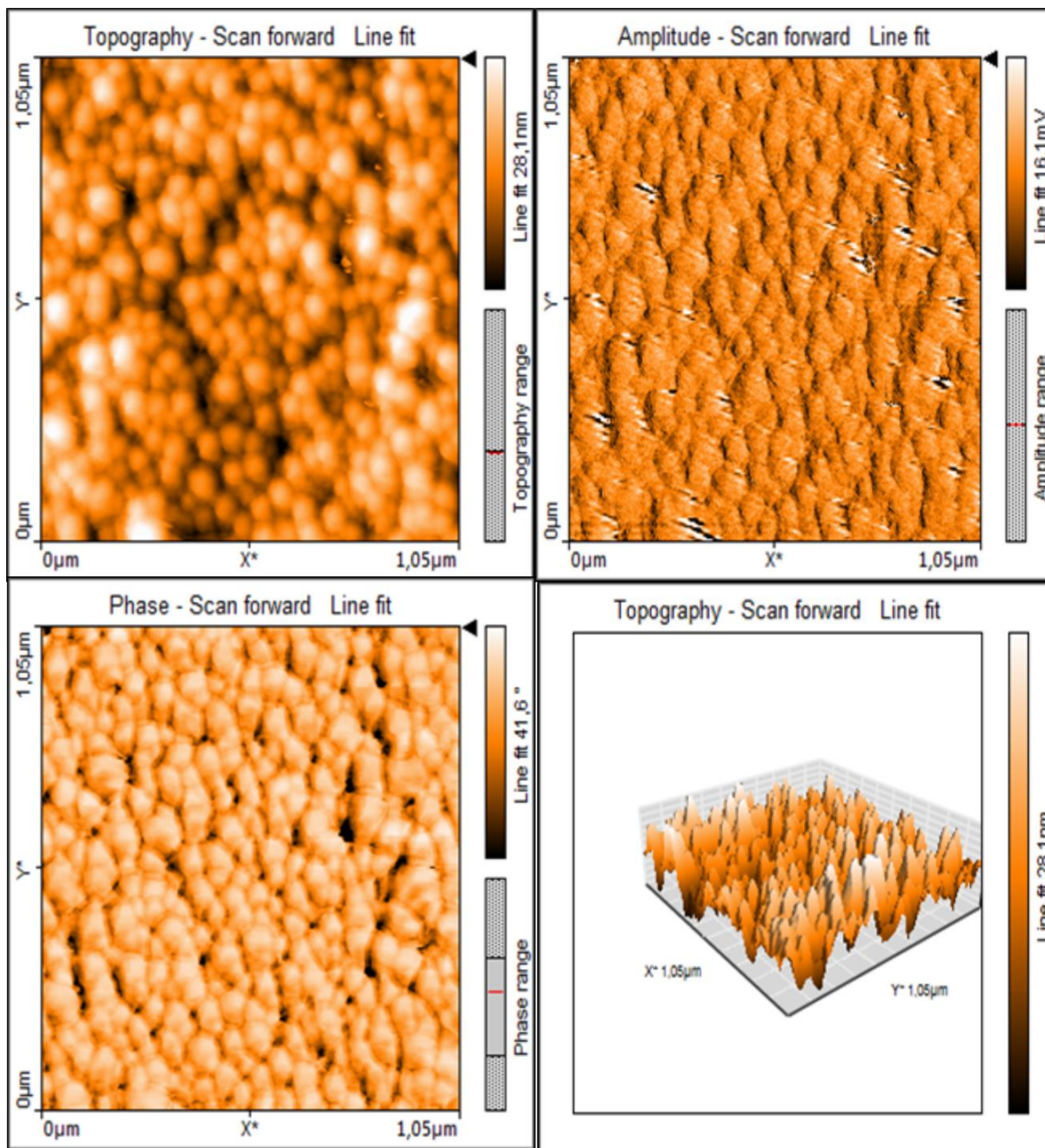


Figure 10. AFM image of P(AN-co-St)/PEDOT nanoparticles 1.03x1.03 μm area on mica glass surface, at 1440 min.

It can be seen from the Fig.9 P(AN-co-St)/PEDOT particles were synthesized homogeneously and also in nanometer dimension with micro emulsion polymerization technique.

Nanoparticles' surface roughness were found from AFM and as seen from Fig.16 roughness of surface of nanoparticles have increasing tendency with time and has maxima about 1440 min. It is attributed that EDOT monomer polymerized on the P(AN-co-St) matrix. It can be also seen that the longer polymerization time cause to decrease of the roughness of nanoparticles.

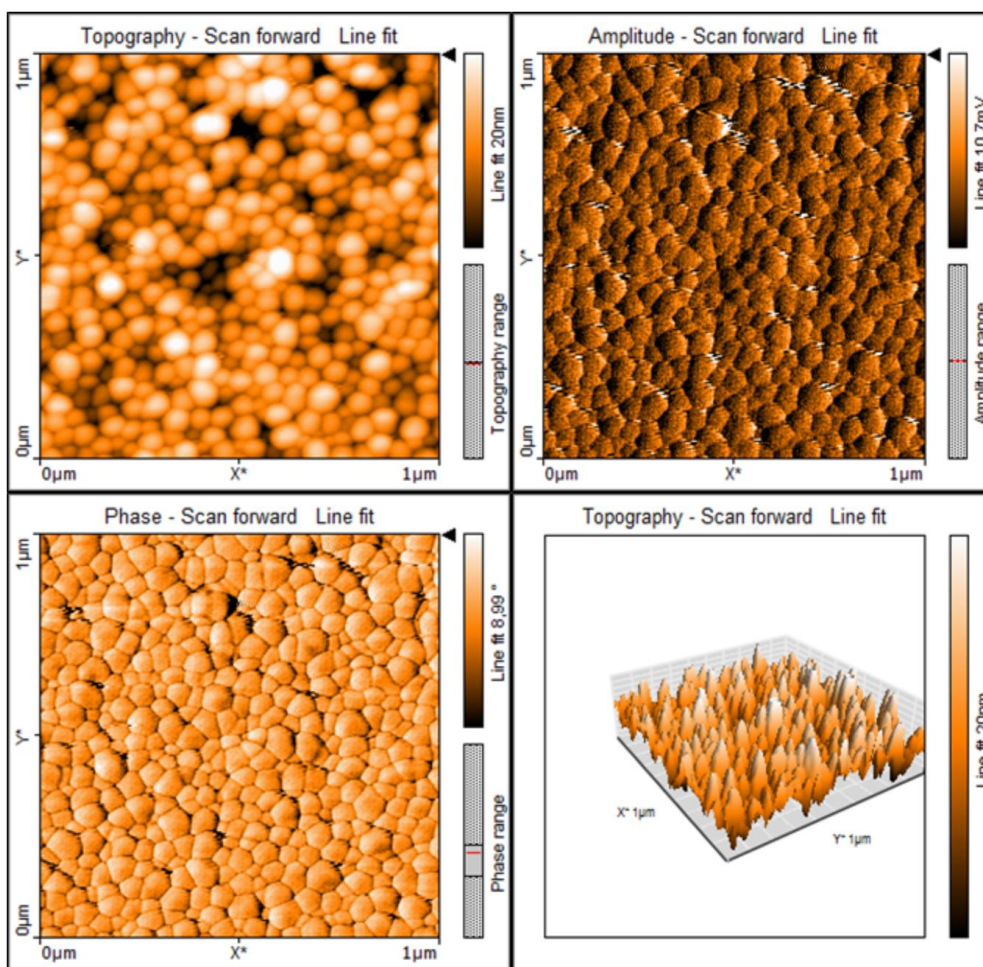


Figure 11. AFM image of P(AN-co-St)/PEDOT nanoparticles 1.03x1.03 μm area on mica glass surface, at 1694 min.

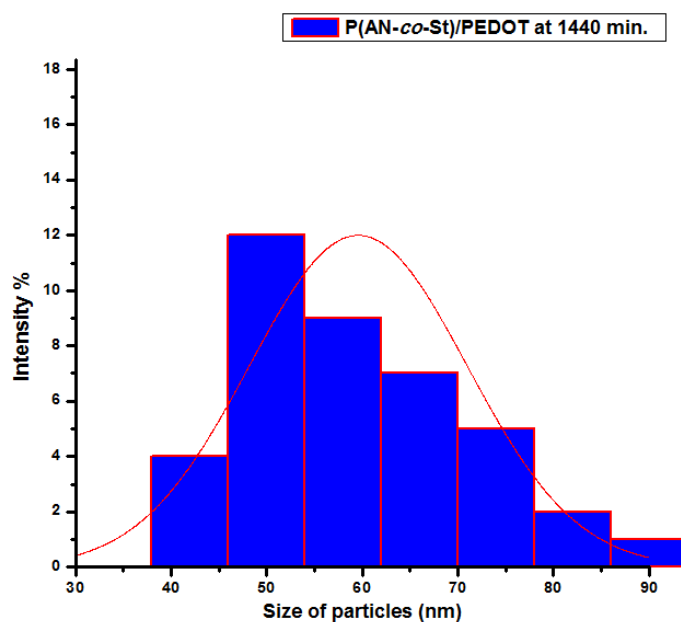


Figure 12. Size of selected nanoparticles from AFM image at 1440 min. of polymerization of P(AN-co-St)/PEDOT measured by image programme.

3.3.2. SEM Studies

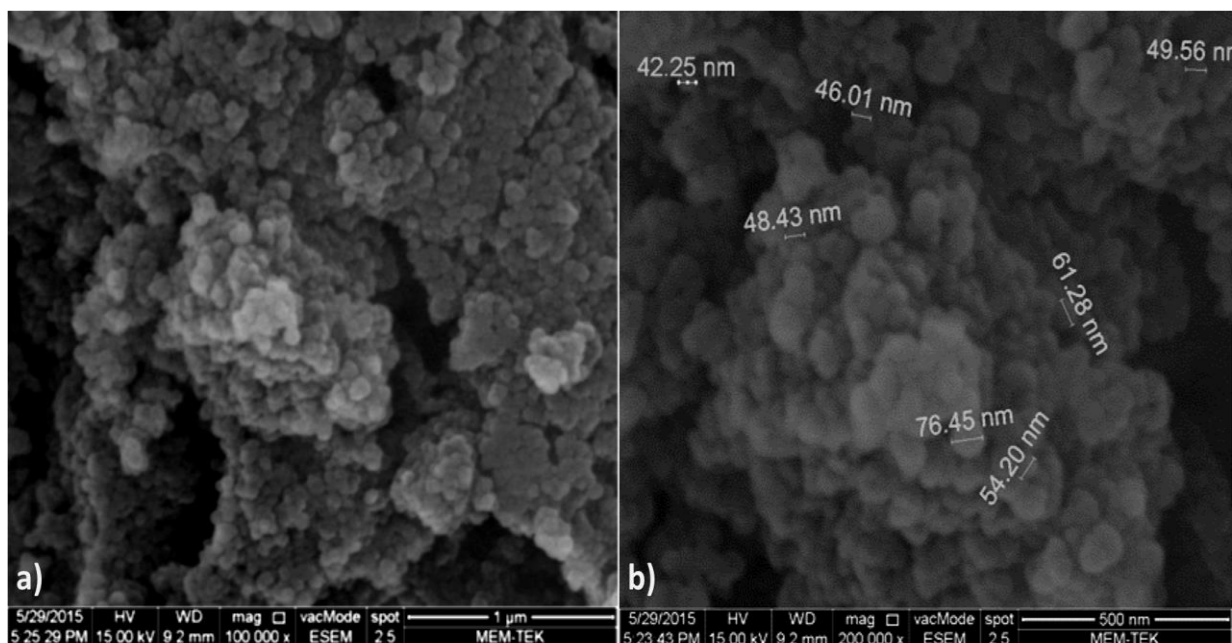


Figure 13. (a) SEM image of P(AN-co-St) matrix nanoparticles in 1 μm ,at 100,000 x magnification (b) SEM image of P(An-co-St) nanoparticles in 500 nm. at 200,000 x magnification

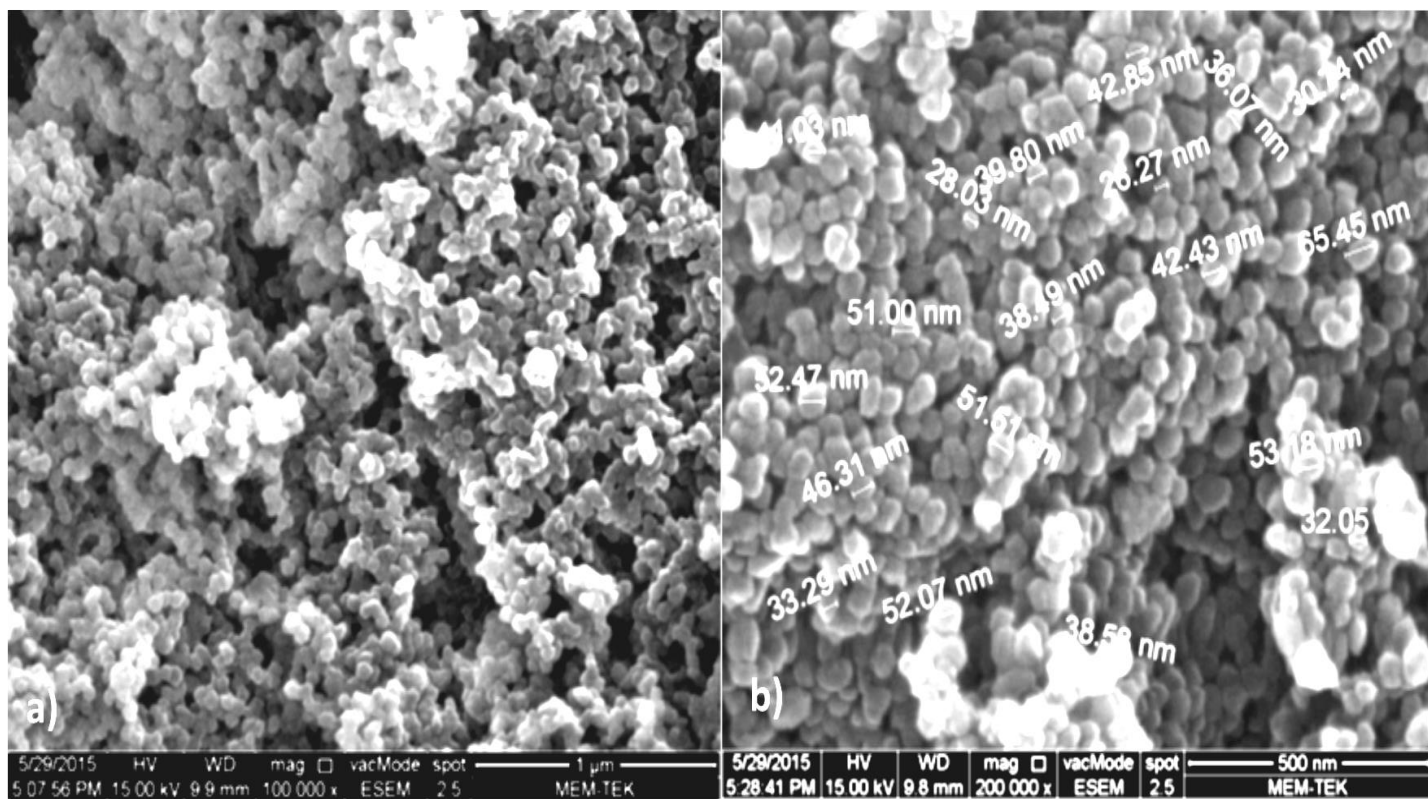


Figure 14. (a) SEM image of P(An-co-St)/PEDOT nanoparticles in 1 μm at 100,000 x magnification. (b) SEM image of P(An-co-St)/PEDOT nanoparticles in 500 nm. at 200,000 x magnification.

The morphologies of particles were studied through SEM. Images were recorded between 100,000 X and 200,000 X magnification, at 15 kV voltage, with a working distance of 9.2 mm.

Fig. 13(a) and (b), Fig. 14(a) and (b) show the SEM images of the P(AN-co-St) matrix and P(AN-co-St)/PEDOT nanoparticles respectively. This SEM images indicate that the P(AN-co-St)/PEDOT nanoparticles were synthesized uniform in size.

The particles of P(AN-co-St) and P(AN-co-St)/PEDOT were uniform in spherical shape. The particles P(AN-co-St) have an average diameter of 40~80 nm and P(AN-co-St)/PEDOT nanoparticles display smallest particle sizes of in the range of 25~65 nm with spherical shapes as calculated approximately from SEM results. The particle size range were obtained from both AFM and SEM matches each other. After the polymerization of EDOT, the surface became rough it is most likely due to recovery from the swollen state throughout the in situ polymerization and drying process and also the integration of PEDOT in the composite.

3.4. Electrochemical Impedance Spectroscopy and Equivalent Circuit Modelling (EIS)

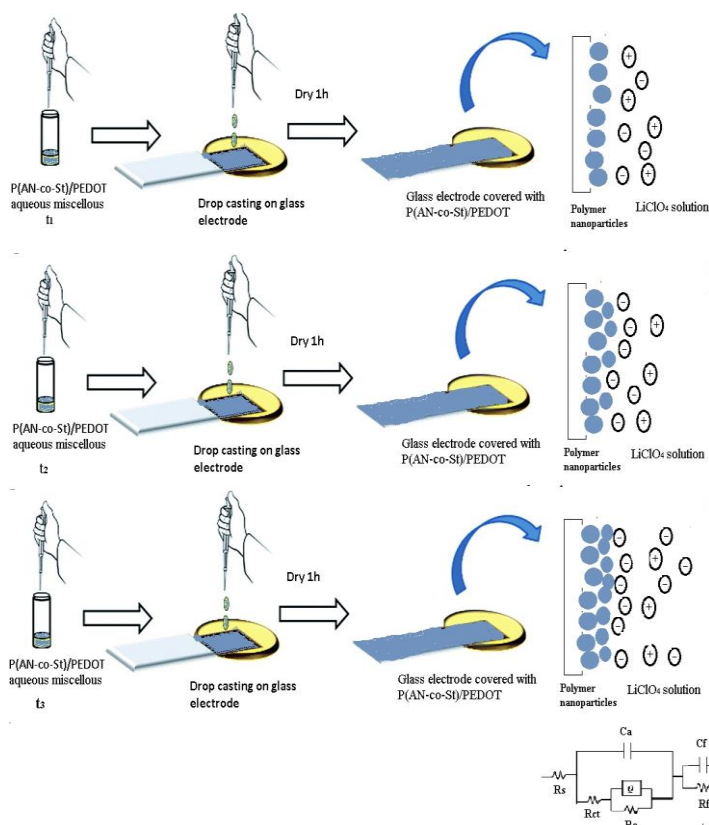


Figure 15. Schematic diagram of electrode fabrication process and equivalent electrical circuit model for the simulation of the EIS spectra of PEDOT covered P(AN-co-St) nanoparticles.

The electrical properties of PEDOT coated P(AN-co-St) nanoparticles on glass were observed by Electrochemical Impedance Spectroscopy. To evaluate electrochemical behaviour and impedance data of P(AN-co-St)/PEDOT nanoparticles, samples were taken from aqueous polymer solution

during in situ emulsion polymerization, in predetermined time intervals (30th, 90th, 180th, 900th and 1440th minute) at room temperature. Fig.15 shows a schematic of the experimental procedure adopted for the preparation of P(AN-co-St)/PEDOT nanofilms using drop casting method. P(AN-co-St)/PEDOT nanofilms were deposited onto glass substrates by drop casting of an aqueous solution of the synthesized P(AN-co-St)/PEDOT. The nanofilms were then dried under vacuum at 60°C for 1 h to vaporize the residual water. The nanofilms were used as working electrodes (Fig.15). The electrical equivalent circuits were chosen to better describe the system properties and to obtain a well fitted data.

The electrical equivalent circuit can support information for the characteristic components of the system and, at the mean time, permit a decision among various potential assumptions about the system. The electrical equivalent circuit $R(C(R(Q(R))))(CR)$ was considered while the electrochemical variables of P(AN-co-St)/PEDOT nanoparticles in the electrolytes were fitted (Fig. 15).

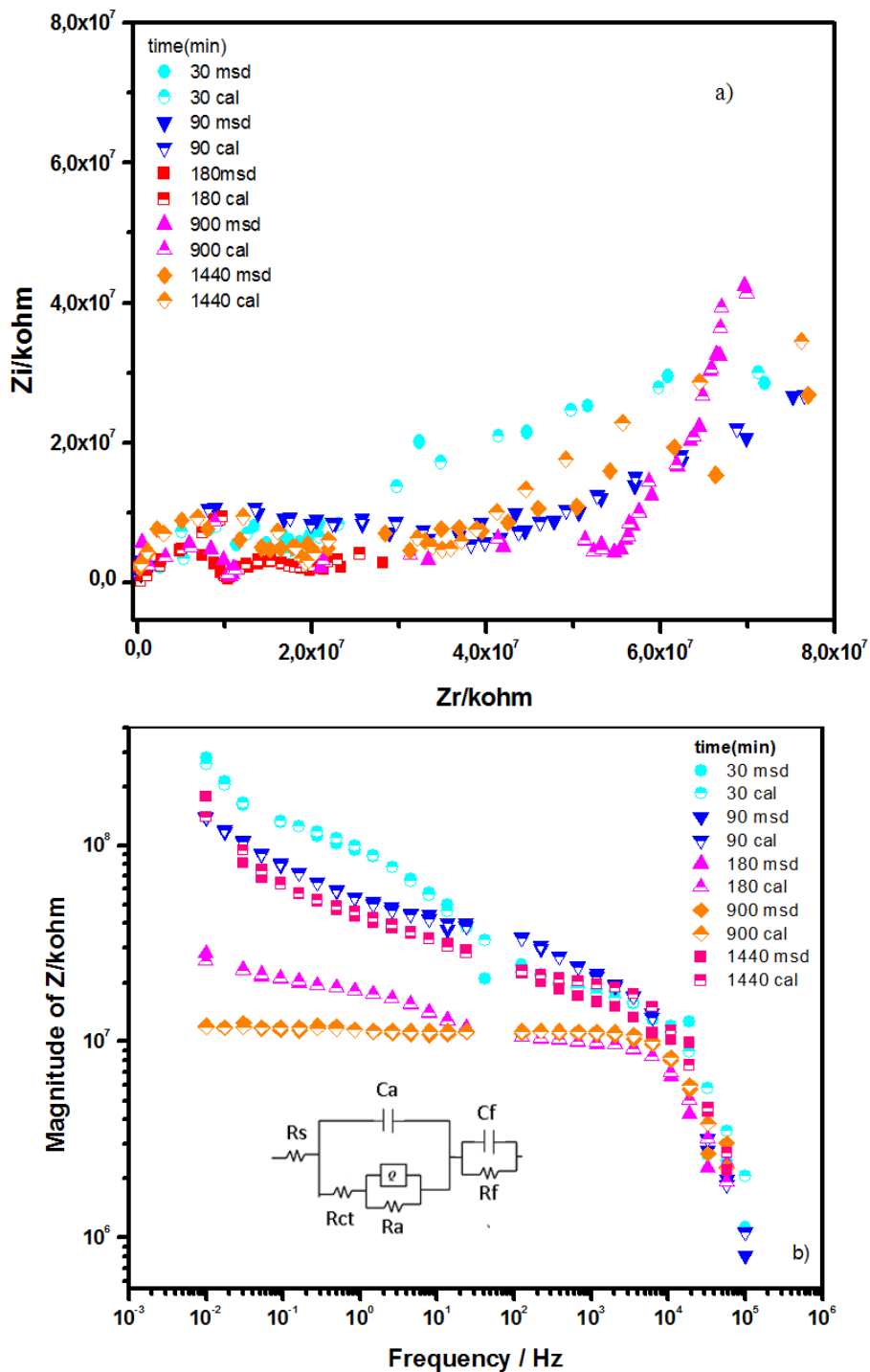
The EEC model is combination of the solvent resistance R_s , the adsorption capacitance and resistance (C_a and R_a), a constant-phase element, (Q), R_{ct} charge transfer resistance (or polarization resistance), R_F and C_F are defined as the resistance and capacitance of the polymer film. The solution resistance (R_s) is defined as the total resistances due to the Ohmic resistance of the solution [20] and electrical contacts [21]. The R_s is ascribed to the solution resistance of the nanocomposites, and the parallel combination of the constant phase element, Q, and the charge transfer resistance between the nanofilms and the electrolyte interface forms second component of the circuit and used as a model for the inhomogeneity in the system [22]. The charging/discharging process on the surface of the film corresponds to R_a and C_a . The solvent resistances of the PEDOT films in the %0.01M $LiClO_4$ supporting electrolyte solutions were higher than the solvent resistances of the P(AN-co-St)/PEDOT in $LiClO_4$ supporting electrolyte solutions for different time intervals. This resulted from the P(AN-co-St) chains in nanoparticles and originating from the variety of the chain lengths, different morphologies, and conductivity of the P(AN-co-St)/PEDOT.

Electron transfer process which is regarding to the exchange current density, inversely can be understood with charge transfer resistance (R_{ct}) Hence, if R_{ct} is lower, it implies a simple interfacial electron transfer process and therefore a higher specific Faradaic(pseudo)capacitance [23]. It is attributed that R_{CT} values decreases during polymerization which indicates the formation of PEDOT nanoparticles on the matrix. The surface morphology of the nanoparticles confirm that a homogeneous structure composed of spherical grains with a porous structure that promotes the charge-transfer process near the electrode/electrolyte surface. Moreover, it has been proven with Electrochemical Impedance Spectroscopy that PEDOT nanoparticles grown on the matrix by time. PEDOT has smaller spherical grains than the P(AN-co-St)/PEDOT film, which is most likely responsible for the difficulties in preserving the connectivity between the pores, which cause the lowest interfacial area for charge transport. In similar studies for the impedance spectroscopy of PEDOT nanoparticles capacitive measurements were performed by using ITO-PET electrode [24]. Herein nanoparticles of P(AN-co-St)/PEDOT, that taken from polymerization solution at indicated time, were coated on glass electrode during polymerization.

The Bode Magnitude plots of the nanoparticles were recorded by applying AC signal of 10 mV amplitude in the frequency range of 0.01 Hz–100 kHz. From the Bode magnitude plot, $|Z|$, which also

termed as absolute impedance, values were taken from 0.01 Hz of low frequency and these values were plotted against to time (Fig. 17 (b)).

As can be seen from Fig. 17, the dependence of impedance and roughness values to polymerization time inversely proportional to each other.



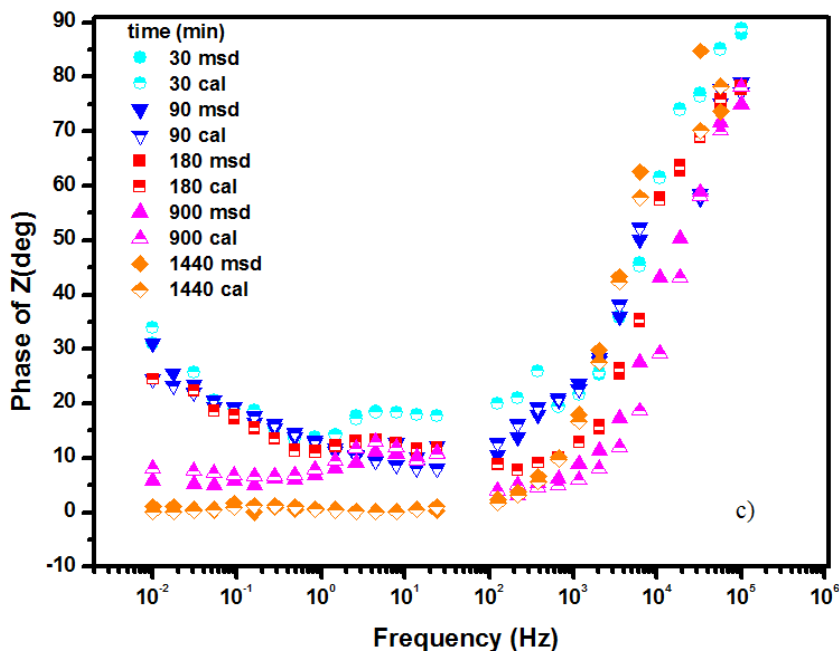


Figure 16. (a) The Nyquist plot, (b) The Bode Magnitude plot, (c) The Bode Phase plot for different time intervals for the P(AN-co-St)/PEDOT.

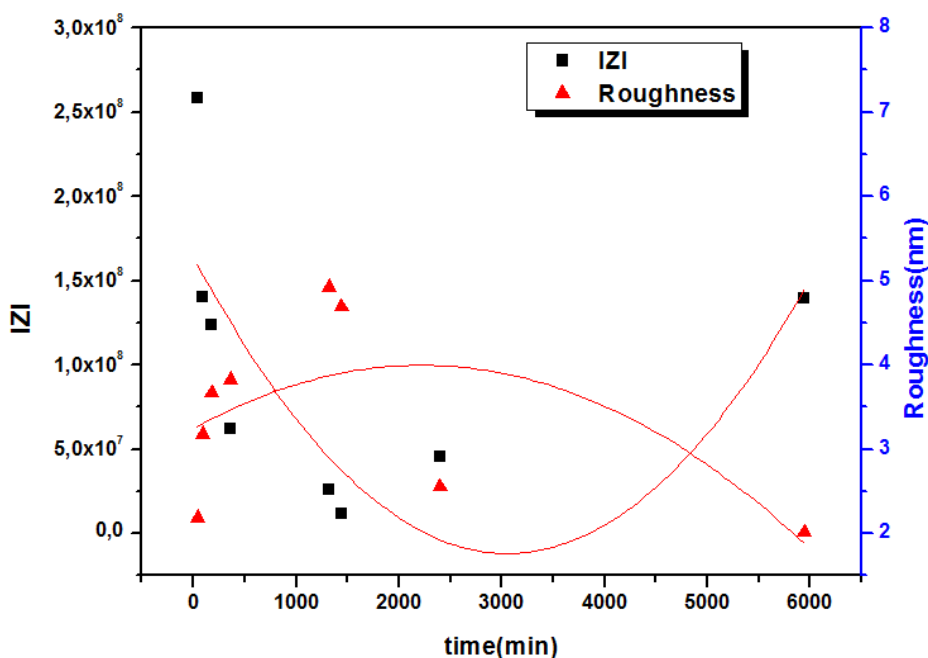


Figure 17. Correlation between absolute impedance |ZI| and Roughness as a function of time for P(AN-co-St)/PEDOT core shell nanoparticles formation.

At the early stages of polymerization, P(AN-co-St) matrix has thin layer of PEDOT nanoparticles, it causes to decreasing of IZI value down to 1440 min (Fig. 17). For longer times of polymerization, after 1440 min., IZI value increase while the roughness of the nanoparticles decrease. It shows that for longer polymerization time excess PEDOT nanoparticles on surface of the matrix peel off and suspended in the aqueous solution.

4. CONCLUSION

The P(AN-*co*-St) core latex with the size of 40–80 nm was obtained by polymerizing with APS as initiator in micro emulsion system at 25°C. These P(AN-*co*-St) nanoparticles prepared in micro emulsion system were successfully coated with PEDOT particles by in situ emulsion polymerization and progress of polymerization followed by time. Electrochemical impedance spectroscopy, ATR-FTIR, UV-Visible spectrophotometric, AFM and SEM approach are used to determine growth of the PEDOT on P(AN-*co*-St) nanoparticles. Moreover, this study provides a simple preparation route for nano-sized with spherical shaped P(AN-*co*-St) matrix covered by PEDOT particles, which enhances its conductivity.

References

1. J. Jang, J.H. Oh, and G.D. Stucky, *Angew. Chem. Int. Ed.*, 41 (2002) 4016.
2. Y. Leia, H. Oohatab, S. Kurodac, S. Sasakid and T. Yamamoto, *Synth. Met.*, 149 (2005) 211.
3. A. Reung-u-Rai, A. Prom-Jun, W. Prissanaroon-Ouajai, and S. Ouajai, *J. Met. Mater. Miner.*, 18 (2008) 27.
4. V. Ovando-Medina, R.D. Peralta, E. Mendizábal, H. Martínez-Gutiérrez, T.E. Lara-Ceniceros, R. Ledezma-Rodríguez, *Colloid. Polym. Sci.*, 289 (2011) 759.
5. F. Yan and G. Xue, *J. Mater. Chem.*, 9 (1999) 3035.
6. J. Stejskal, M. Omastova, S. Fedorova, J. Prokes, M. Trchova, *Polymer* 44 (2003) 1353.
7. F. Yan, C. Zheng, X. Zhai, D. Zhao, *J. Appl. Polym. Sci.*, 67 (1998) 747.
8. S.M. Jin, Y.T. Joo, Y.J. Park, Y. Kim, *J. Appl. Polym. Sci.*, 121 (2011) 1442.
9. C. DeArmitt, S.P. Armes, *Langmuir*, 9 (1993) 652.
10. C.O. Oriakhi and M.M. Lerner, *Mater. Res. Bull.*, 30 (1995) 723.
11. Y. Kudoh, *Synth. Met.*, 79 (1996) 17.
12. Y. Kudoh, K. Akami and Y. Matsuya, *Synth. Met.*, 98 (1998) 65.
13. M.A. Khan, and S.P. Armes, *Langmuir*, 15 (1999) 3469.
14. M.G. Han, S.H. Foulger, *Chem. Commun.*, 24 (2004) 2514.
15. J.W. Choi, M.G. Han, Y.S. Kim, S.G. Oh, S.S. Im, *Synth. Met.* 141 (2004) 293.
16. W.W. Chiu, J. Travařs-Sejdić, R.P. Cooney, G.A. Bowmaker, *Synth. Met.* 155 (2005) 80.
17. S.A. Sarac, G. Sonmez and F.C. Cebeci, *J. Appl. Electrochem.*, 33 (2003) 295.
18. B. Massoumi, N. Alipour, S. Fathalipour and M. Jaymand, *High Perform. Polym.*, 27 (2015) 161
19. B. Winther-Jensen, K. West, *React. Funct. Polym.* 66 (2006) 479.
20. D. Giray, T. Balkan, B. Dietzel and A.S. Sarac, *Eur. Polym. J.*, 49 (2013) 2645.
21. Z. Guler, P. Erkoc, and A.S. Sarac, *Mater. Express*, 5 (2015) 269.
22. Z. Guler, A.S. Sarac, *Express Polym. Lett.*, 10 (2016) 96.
23. R. Ramya, R. Sivasubramanian, M.V. Sangaranarayanan, *Electrochim. Acta*, 101 (2013) 109.
24. Y. Chen, J. Xu, M. Yunwu, et al., *Mat. Sci. and EngB.*, 178 (2013) 1152.